

# Diagnostic accuracy of late iodine enhancement on cardiac computed tomography with a denoise filter for the evaluation of myocardial infarction

Takuya Matsuda<sup>1</sup> · Teruhito Kido<sup>1</sup> · Toshihide Itoh<sup>2</sup> · Hideyuki Saeki<sup>3</sup> · Susumu Shigemi<sup>3</sup> · Kouki Watanabe<sup>3</sup> · Tomoyuki Kido<sup>4</sup> · Shoji Aono<sup>4</sup> · Masaya Yamamoto<sup>4</sup> · Takeshi Matsuda<sup>5</sup> · Teruhito Mochizuki<sup>1</sup>

Received: 9 July 2015 / Accepted: 16 July 2015 / Published online: 23 July 2015  
© Springer Science+Business Media Dordrecht 2015

**Abstract** We evaluated the image quality and diagnostic performance of late iodine enhancement (LIE) in dual-source computed tomography (DSCT) with low kilo-voltage peak (kVp) images and a denoise filter for the detection of acute myocardial infarction (AMI) in comparison with late gadolinium enhancement (LGE) magnetic resonance imaging (MRI). The Hospital Ethics Committee approved the study protocol. Before discharge, 19 patients who received percutaneous coronary intervention after AMI underwent DSCT and 1.5 T MRI. Immediately after coronary computed tomography (CT) angiography, contrast medium was administered at a slow injection rate. LIE-CT scans were acquired via dual-energy CT and reconstructed as 100-, 140-kVp, and mixed images. An iterative three-dimensional edge-preserved smoothing filter was applied to the 100-kVp images to obtain denoised 100-kVp images. The mixed, 140-kVp, 100-kVp, and denoised 100-kVp images were assessed using contrast-to-noise ratio (CNR), and their diagnostic performance in comparison with MRI and infarcted volumes were evaluated. Three hundred four segments of 19 patients were

evaluated. Fifty-three segments showed LGE in MRI. The median CNR of the mixed, 140-, 100-kVp and denoised 100-kVp images was 3.49, 1.21, 3.57, and 6.08, respectively. The median CNR was significantly higher in the denoised 100-kVp images than in the other three images ( $P < 0.05$ ). The denoised 100-kVp images showed the highest diagnostic accuracy and sensitivity. The percentage of myocardium in the four CT image types was significantly correlated with the respective MRI findings. The use of a denoise filter with a low-kVp image can improve CNR, sensitivity, and accuracy in LIE-CT.

**Keywords** Acute myocardial infarction · Cardiac computed tomography · Image postprocessing · Late iodine enhancement

## Introduction

The assessment of myocardial viability is important in patients with coronary artery disease (CAD), including those with myocardial infarction. Late gadolinium enhancement (LGE) in cardiac magnetic resonance imaging (MRI) is well-correlated with the histopathological findings of infarcted myocardium [1]. Assessments of LGE in cardiac MRI before coronary revascularization can reveal reversible myocardial dysfunction [1–3]. This is an important indicator, since revascularization for irreversibly damaged myocardium cannot improve left ventricular function, potentially subjecting the patient to an unnecessary invasive procedure. Therefore, LGE-MRI is generally used to evaluate the viability of the myocardium. However, MRI is contraindicated in patients with metal implants, pacemakers, and claustrophobia, as well as in patients who cannot be at risk of heart failure. Among the available alternative methods, nuclear

✉ Takuya Matsuda  
tmatsuda.singing@gmail.com

<sup>1</sup> Department of Radiology, Ehime University Graduate School of Medicine, Shitsukawa, Toon, Ehime 791-0295, Japan

<sup>2</sup> Research and Collaboration, Siemens Japan, Shinagawa, Tokyo, Japan

<sup>3</sup> Department of Cardiology, Saiseikai Matsuyama Hospital, Matsuyama, Ehime, Japan

<sup>4</sup> Department of Radiology, Saiseikai Matsuyama Hospital, Matsuyama, Ehime, Japan

<sup>5</sup> Department of Radiology, Matsuyama Red Cross Hospital, Matsuyama, Ehime, Japan

imaging and echocardiography provide some information about the myocardium and its viability, although these techniques have a lower spatial resolution and tissue characterization ability in comparison with MRI [4, 5].

Coronary computed tomography (CT) angiography (CCTA) is a widely available and accepted noninvasive clinical tool because of its very high negative predictive value for CAD [6, 7]. In evaluations of late myocardial enhancement, several studies have reported that CT depict late iodine enhancement (LIE) [8–11]. However, the contrast-to-noise ratio (CNR) is reportedly lower in LIE-CT images than in LGE-MRI [9]. In a porcine model of histopathological infarction, the sensitivity of LIE-CT images at 100-kilovoltage peak (kVp) was lower than that of the LGE-MR images [10]. This lower CNR is one reason for the lower sensitivity in LIE-CT.

The use of dual-energy CT (DECT) enables the comparison of images obtained at different kVp values in the same patient [12, 13]. Thus, to improve the sensitivity of LIE-CT, we established a protocol that employs a bolus and an additional injection using DECT. In addition, to reduce the image noise on 100-kVp images, we developed an iterative three-dimensional (3D) edge-preserved smoothing filter operating on the MATLAB platform. This filter was applied to the 100-kVp images, and a mixed image, a high-kVp image, a low-kVp image, and a denoised low-kVp image were evaluated.

The purpose of this study was to evaluate the image quality and diagnostic performance of LIE on dual-source CT (DSCT) with the use of a denoise filter and a low-kVp image and to compare this LIE-CT approach with LGE-MRI assessments.

## Materials and methods

### Study population

We included adult patients older than 40 years who presented to our hospital between March 2009 and December 2013 with acute myocardial infarction (AMI) for which they underwent emergency percutaneous coronary intervention (PCI) and who provided informed consent. We excluded patients with (1) heart dysfunction greater than a first-degree atrioventricular block; (2) a history of coronary artery bypass graft; (3) chronic atrial fibrillation; (4) cardiac myopathy; (5) renal insufficiency (serum creatinine > 1.5 mg/dL or estimated glomerular filtration rate < 60 mL/min per 1.73 m<sup>2</sup>); (6) pregnancy, hyperthyroidism, or a known allergic reaction to contrast media; (7) New York Heart Association class IV congestive heart failure; or (8) a known history of bronchial asthma.

The study protocol was approved by the hospital ethics committee, and informed consent was obtained from all

patients after emergency PCI. A total of 20 patients were prospectively recruited, and one patient was excluded because of concurrent cardiac sarcoidosis. The remaining 19 patients (aged 46–88 years,  $66.9 \pm 11.5$  years; 13 men) underwent CCTA, contrast-enhanced dual-energy LIE-CT, and LGE-MRI.

### DECT protocol

Figure 1 shows the DECT protocol. Patients were scanned in a fasting state in the supine position. The nonionic contrast medium iopamidol (Iopamiron; Bayer Yakuhin Ltd., Osaka, Japan; 350 or 370 mgI/mL) was used. After the test injection (10 mL of contrast medium), the contrast medium (0.7 mL/kg) was injected at a rate of 5 mL/s through a 20-G intravenous antecubital cannula, followed by a 20-mL injection of saline using a dual-syringe injector (Dual Shot Alpha; Nemoto Kyorindo, Tokyo, Japan). Contrast enhancement in the descending aorta was monitored. After the enhancement reached the descending aorta [the CT value threshold was 150 Hounsfield units (HU)], CCTA scanning was performed during breath-holding. Immediately after the CCTA, an additional intravenous injection of contrast medium with a slow injection rate (50 mL, 12 mL/min) was administered, and an LIE-CT scan was performed in dual-energy mode 5 min after CCTA scanning.

The chosen dual-source CT systems (SOMATOM Definition and SOMATOM Definition Flash, Siemens Healthcare, Forchheim, Germany) were equipped with two X-ray tubes and two detector arrays mounted in the same gantry. In 2009, two patients underwent DECT with the Definition; from 2010 to 2013, 17 patients underwent DECT with the Definition Flash. The gantry rotation and collimation for the Definition were 330 ms and  $64 \times 0.6$  mm, respectively, while the corresponding values for the Definition Flash were 275 ms and  $128 \times 0.6$  mm, respectively. The pitches were 0.2 (for a heart rate <60 beats/minute), 0.25 (heart rate of 61–70 beats/minute), 0.3 (heart rate of 71–80 beats/minute), and 0.35 (heart rate greater than 81 beats/minute) with the Definition and 0.22 (heart rate less than 60 beats/minute), 0.25 (heart rate of 61–70 beats/minute), 0.29 (heart rate of 71–80 beats/minute), and 0.32 (heart rate greater than 81 beats/minute) with the Definition Flash. When using the Definition, one tube of the dual-source system was operated with 90 mAs at 140 kV, and the other tube was operated with 180 mAs at 100 kV. When using the Definition Flash, one tube of the dual-source system was operated with 157 mAs at 140 kV, with a tin (Sn) filter for optimization of the X-ray spectrum, and the other tube was operated with 185 mAs at 100 kV. The data were acquired in the craniocaudal direction with simultaneous recording of the patient's electrocardiogram

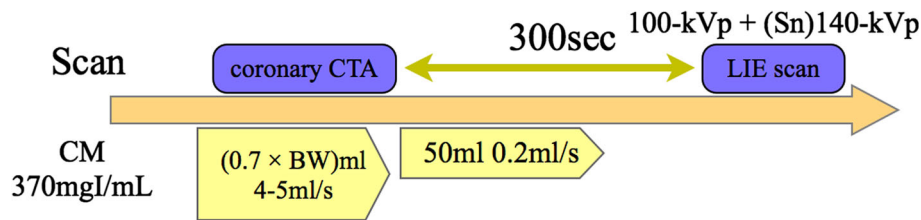


**Fig. 1** The cardiac CT protocol. After coronary CT angiography (CTA), an additional contrast medium is added at a slow injection rate. The late iodine enhancement CT is then performed 300 s after

the coronary CT. *BW* body weight, *CM* contrast medium, *kVp* kilovoltage peak, *LIE* late iodine enhancement

(ECG) signal in order to enable retrospective registration of the reconstructed images to the desired cardiac phase. The anatomical range extended from the level of the bronchial bifurcation to just below the dome of the diaphragm.

### LGE-MRI imaging protocol

A 1.5-T MRI unit (Signa Excite; GE Healthcare UK, Ltd., Buckinghamshire, England) was used for LGE-MRI, employing a four-channel cardiac array and prospective ECG triggering. The gadolinium-based contrast medium gadopentetate dimeglumine (Magnevist; Bayer Yakuhin Ltd., Osaka, Japan; 0.1 mmol/kg) was injected through a 22-G intravenous antecubital cannula. Fifteen min after administering the contrast medium, LGE-MR images were obtained using an inversion recovery prepared two-dimensional fast gradient echo sequence. Imaging parameters were as follows: repetition time, 6.8 ms; echo time, 3.18 ms; inversion time, 200–300 ms (adjusted to the null signal of the normal myocardium); section thickness 8–14 mm; field of view, 360 mm; matrix size 256 × 192; echo train length, 1; view per segment, 24; flip angle, 20°; and band width, 31.3 kHz.

### LIE-DECT image post-processing

From the DECT datasets, four different image series were obtained: (1) the mixed images, (2) the 140-kVp images, (3) the 100-kVp images, and (4) the denoised 100-kVp images. Using 1-mm-thick slices, images at two kVp values (140 and 100 kVp) were reconstructed in the phase least affected by motion. These two-image series were loaded into the dedicated dual-energy application (Syngo Dual-Energy software; Siemens Healthcare, Forchheim, Germany). The mixed image was reconstructed by linearly blending the 140-kVp image and the 100-kVp image. The weighting factor was 0.5 (i.e., the mixed image was obtained from 50 % of the 140-kVp spectrum and 50 % of the 100-kVp spectrum).

To improve sensitivity of the 100-kVp image by reducing image noise, we developed an iterative 3D edge-

preserving program running on MATLAB (Mathworks, Natick, MA, USA). The filter was based on an anisotropic diffusion equation filter, which allowed smoothing of noise along edges, such as organ contours, and enhancement of the edge itself in order to increase image contrast [14]. Our algorithm detected the strength of edges in a cubic region of  $5 \times 5 \times 5$  voxels by comparing differences in pixel values along the nine directions including the center voxels, then applied a type of Gaussian low pass filter for each direction, with different smoothing levels corresponding to the strength of the edge. This process was applied to all voxels in the data volume. To avoid unwanted artificial image depiction, we applied the Gaussian low pass filter with the weakest possible setting while repeating the filtering with a fixed number of iterations (9 times in our software). As a result, we obtained images with low pixel noise but without degradation of organ contours or image contrast. We applied the filter to the 100-kVp images in order to obtain the denoised 100-kVp images.

The typical left ventricular short-axis views were obtained from the mixed images, the 140-kVp images, the 100-kVp images, and the denoised 100-kVp images using a workstation (Ziostation 2; Ziosoft, Inc., Tokyo, Japan) for multiplanar reconstruction. The slice thickness was set at 8 mm.

### Image analyses

#### Contrast-to-noise ratio

To evaluate the image quality of the CT series, we calculated the CNRs for the cases that were detected by LGE on MRI. The radiologists used the LGE-MR images as a reference for detecting abnormal areas. A region of interest (ROI) larger than  $1.0 \text{ cm}^2$  was drawn on the normal myocardium, and the mean CT value and standard deviation (SD) were calculated. Another ROI fitted to LIE was drawn manually, and the mean CT value was calculated.

“Contrast” was defined as the difference in mean CT value between the LIE and normal myocardium. “Noise” was defined as the SD of the normal myocardium. The

CNRs were calculated by dividing the contrast by the noise. Contrast, noise, and CNR were calculated three times for each patient, and the mean value was used for analysis. All ROIs were copied and pasted at the same location on each image.

### *Diagnostic accuracy*

One experienced cardiac radiologist who was not involved in the LIE-DECT reading and was blinded to all patient-related data independently evaluated the left ventricular short-axis LGE-MR image. The left ventricular myocardial segments were based on a standard 16-segment model (the apex was excluded from the American Heart Association's 17-segment model [15]). The subintimal or transmural area that showed signal hyperintensity in comparison with the normal surrounding myocardium was defined as LGE.

Two experienced cardiac radiologists independently evaluated the LIE-CT series. The left ventricular myocardial segments were based on a standard 16-segment model. Four different images were evaluated in random order. The subintimal or transmural area that showed signal hyperdensity in comparison with the normal surrounding myocardium was defined as LIE.

### *The volume of late enhancement*

To evaluate the correlation between MRI and CT findings, another radiologist calculated the volume of late enhancement. The areas of the left ventricular myocardium and late enhancement were calculated by drawing ROIs. The volume was calculated by multiplying the summed area by the slice thickness, and percent myocardium was defined as the percentage of late enhancement volume in the left ventricular myocardium volume. The percent myocardium was calculated in the LGE-MR image, mixed image, 140-kVp image, 100-kVp image, and denoised 100-kVp image.

### **Statistical analyses**

The Friedman test was used for assessments of contrast, noise, and CNR in order to compare the image quality of the mixed, 140-, 100-kVp, and denoised 100-kVp images. For the LIE-CT images (i.e., mixed image, 140-kVp image, 100-kVp image, and denoised 100-kVp image), the sensitivity, specificity, positive predictive value, negative predictive value, and accuracy for detecting late enhancement areas in the left ventricular myocardium were calculated, using the LGE-MRI findings as the standard of reference. Spearman's correlation coefficients between the percent myocardium of MRI and that of each CT image were calculated. Bland–Altman plots were drawn based on the

percent myocardium of the MRI and the percent myocardium of each CT image.

All statistical analyses were performed using SPSS software, version 19 (SPSS, Chicago, IL, USA). A probability value less than 0.05 was considered statistically significant.

### **Results**

All 19 patients completed the cardiac LGE-MRI and LIE-CT examinations without severe complications. Table 1 shows the patients' characteristics. The average effective dose for patients undergoing LIE-CT was  $7.00 \pm 2.81$  mSv. The average effective dose for the 100- and 140-kVp images was  $3.91 \pm 1.71$  mSv and  $3.09 \pm 1.21$  mSv, respectively.

### **CNR**

Figure 2 shows the box plot of the contrast, noise, and CNR. The median contrast (interquartile range) of the mixed, 140-, 100-kVp, and denoised 100-kVp images was 21.53 HU (16.99–24.69 HU), 9.28 HU (7.11–12.98 HU), 34.43 HU (26.73–36.34 HU), and 31.42 HU (24.81–34.25 HU), respectively. The median noise (interquartile range) of the mixed, 140-, 100-kVp, and denoised 100-kVp images was 5.97 HU (5.07–7.26 HU), 7.23 HU (6.01–8.44 HU), 8.10 HU (7.27–9.70 HU), and 4.23 HU (3.58–5.44 HU), respectively. The median CNR (interquartile range) of the mixed, 140-, 100-kVp, and denoised 100-kVp images was 3.49 (2.30–4.78), 1.21 (0.61–1.95), 3.57 (2.90–4.68), and 6.08 (4.83–9.09), respectively. The median CNR of the denoised 100-kVp images was significantly higher than those of the other three types of images. Figure 3 shows a representative image with sufficiently reduced noise.

### **Diagnostic accuracy**

All 304 segments were assessed. One patient was diagnosed as showing no late enhancement both in MRI and CT. Late gadolinium enhancement was detected in 53 (17 %) segments in LGE-MRI. Late iodine enhancement was detected in 46 (15 %) mixed images, 28 (9 %) 140-kVp images, 52 (17 %) 100-kVp images, and 53 (17 %) denoised 100-kVp images. Table 2 summarizes the diagnostic accuracies. The denoised 100-kVp image had the highest sensitivity and accuracy.

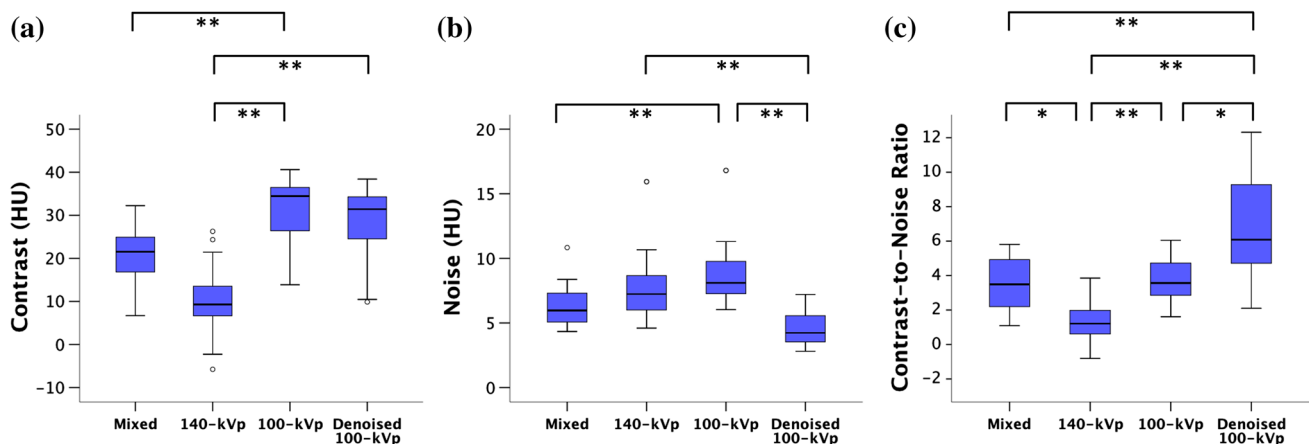
### **Volume of late enhancement**

The median percent myocardium (interquartile range) of LGE-MRI was 5.54 % (4.18–9.79 %). The median percent

**Table 1** Patient characteristics ( $n = 19$ )

Characteristics	Values
Age, mean (SD) [minimum, maximum], years	67 (12) [46, 88]
Male sex, n (%)	14 (74)
Number of days between CT and MRI, mean (SD), days	3 (3)
<i>Risk factors, n (%)</i>	
Hypertension	14 (74)
Dyslipidemia	10 (53)
Diabetes mellitus	4 (21)
Smoking	6 (32)
Positive family history	1 (5)
<i>Examination characteristics</i>	
SOMATOM Definition Flash, n (%)	17 (89)
<i>Radiation dose</i>	
DECT effective dose, mean (SD), mSv	7.00 (2.81)
100 kV effective dose, mean (SD), mSv	3.91 (1.71)
(Sn) 140 kV effective dose, mean (SD), mSv	3.09 (1.21)

DECT dual-energy CT, SD standard deviation

**Fig. 2** Comparison of (a) contrast, (b) noise, and (c) contrast-to-noise ratio (CNR) for mixed, 140-, 100-kVp, and denoised 100-kVp images. The median CNR of the denoised images is significantly higher than those of the mixed, 140-, and 100-kVp images. \* $P < 0.05$ ; \*\* $P < 0.001$ 

myocardium (range) was 5.72 % (3.41–9.15 %) in the mixed images, 3.31 % (1.74–5.41 %) in the 140-kVp images, 5.09 % (2.55–6.46 %) in the 100-kVp images, and 5.59 % (3.40–10.29 %) in the denoised 100-kVp images. The percent myocardium values of the 140- and 100-kVp images were significantly lower than that of the LGE-MR images ( $P < 0.05$ ).

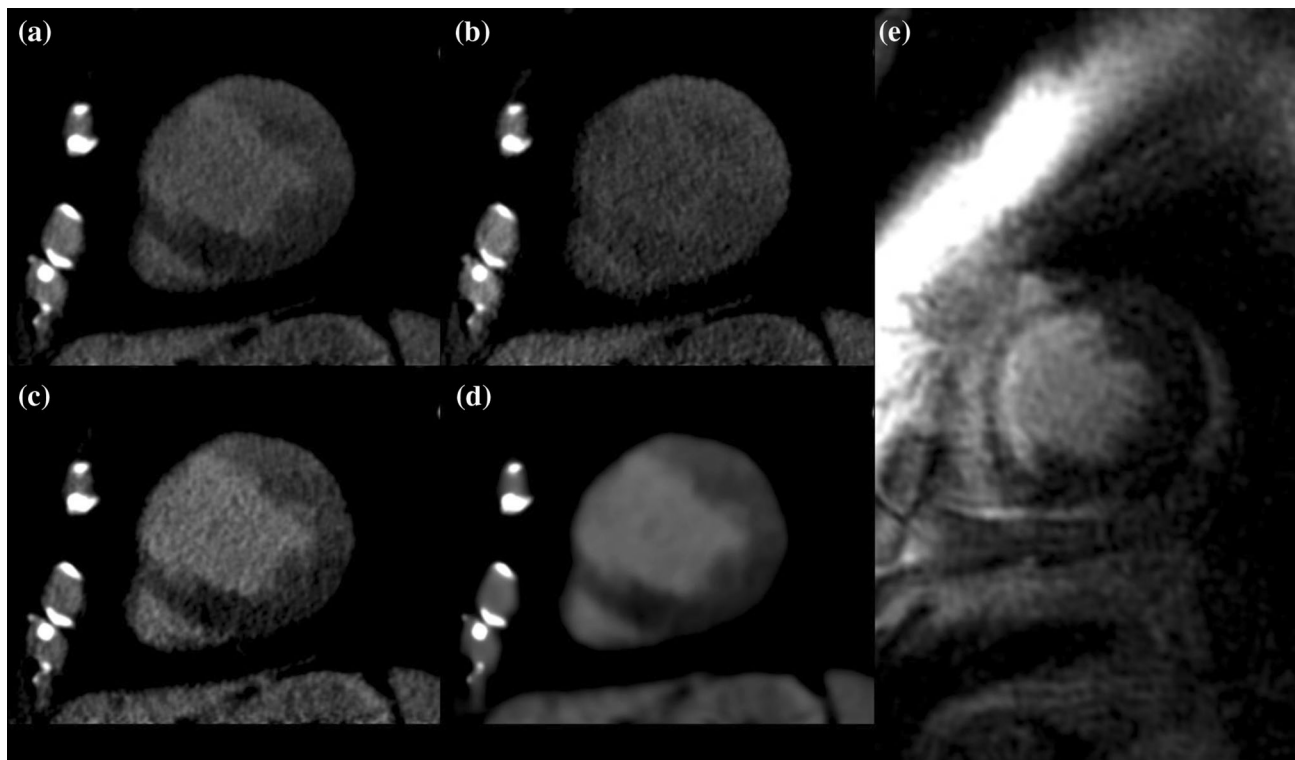
The percent myocardium of each LIE-CT image was well correlated with the percent myocardium of the LGE-MR images (Fig. 4). Spearman's correlation coefficients between the percent myocardium of the mixed, 140-, 100-kVp, and denoised 100-kVp images and that of the respective MR images were 0.937, 0.907, 0.775, and 0.846, respectively.

Figure 4 shows the Bland–Altman plots. The mean difference of the mixed, 140-, 100-kVp, and denoised 100-kVp images from MRI was 0.41, 2.74, 1.38, and 0.53,

respectively. The limit of agreement of the mixed, 140-, 100-kVp and denoised 100-kVp images from MRI ranged from  $-2.62$  to  $3.44$ ,  $-0.50$  to  $5.98$ ,  $-3.53$  to  $6.30$ , and  $-3.28$  to  $4.33$ , respectively.

## Discussion

We evaluated four different LIE-CT image series (mixed, 140-, 100-kVp, and denoised 100-kVp images) in patients with AMI using DECT and compared different kVp images and mixed images. To our knowledge, this is the first clinical study to evaluate LIE in patients with AMI using DECT. We evaluated CNR, diagnostic accuracy, and percent myocardium in mixed, 140-, 100-kVp, and denoised 100-kVp images.



**Fig. 3** Late enhancement CT and MR images in a woman in her 70 s with acute myocardial infarction. (a) The mixed image, (b) the tin (Sn) 140-kVp image, (c) the 100-kVp image, and (d) the denoised 100-kVp image of late enhancement CT, and (e) the late enhancement

MR image. The denoised 100-kVp image (d) has high contrast and low noise. In the denoised image, late iodine enhancement is easily detected on MRI in the same segment as late gadolinium enhancement

**Table 2** Segment-based diagnostic performance

	Sensitivity	Specificity	PPV	NPV	Accuracy
Mixed	71.7 % (59.6–83.8)	96.8 % (94.6–99.0)	82.6 % (71.7–93.6)	94.2 % (91.3–97.0)	92.4 % (89.5–95.4)
140-kVp	28.3 % (16.2–40.4)	94.8 % (92.1–97.6)	53.6 % (35.1–72.0)	86.2 % (82.2–90.3)	83.2 % (79.0–87.4)
100-kVp	79.2 % (68.3–90.2)	96.0 % (93.6–98.4)	80.8 % (70.1–91.5)	95.6 % (93.1–98.2)	93.1 % (90.2–95.9)
Denoised 100-kVp	81.1 % (70.6–91.7)	96.0 % (93.6–98.4)	81.1 % (70.6–91.7)	96.0 % (93.6–98.4)	93.4 % (90.6–96.2)

All values are % (95 % confidence intervals)

NPV negative predictive value, PPV positive predictive value

The median CNR of the denoised 100-kVp images was the highest and was significantly higher than those of the other three types of images. We found that the 100-kVp images had a higher sensitivity and accuracy than the mixed and 140-kVp images. This finding is consistent with past reports on DECT [12, 13]. In addition, we found that the denoised 100-kVp images had higher sensitivity and accuracy than the 100-kVp images. The percent myocardium of each LIE-CT image was well correlated with that of the LGE-MR images. The Bland–Altman plot did not show an extreme distribution in the limit of agreement. In our results, the difference in effective dose between the

100- and 140-kVp images was not high because the value of each tube current was set such that it could obtain images with similar noise levels (Definition values were 90 mAs at 140 kV and 180 mAs at 100 kV; Definition Flash values were 157 mAs at 140 kV with a tin filter and 185 mAs at 100 kV). In DECT, small differences in image noise between the two images are important in order to obtain proper mixed images. In fact, the difference in noise between the 100- and 140-kVp images was not significant in our results (see Fig. 2).

Several studies have reported that CT is able to depict LIE [8–10]. However, comprehensive cardiac CT

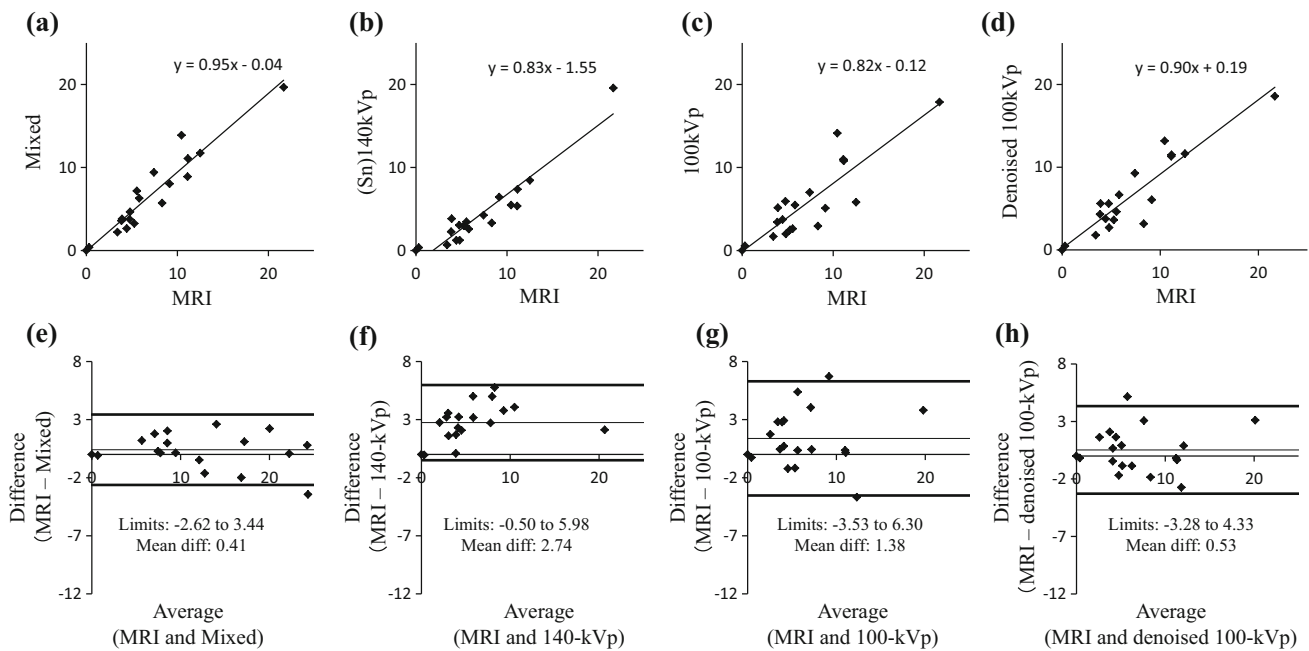


**Fig. 4** Correlation chart of MRI and the (a) mixed image, (b) 140-kVp image, (c) 100-kVp image, and (d) denoised 100-kVp image. The Bland-Altman plot of MRI and the (e) mixed image, (f) 140-kVp image, (g) 100-kVp image, and (h) denoised 100-kVp image

examinations (which include calcium scoring, CCTA, perfusion CT, and LIE-CT) require a relatively high radiation dose if they are performed without a control. Thus, a low radiation dose is also required in LIE-CT. One approach to reduce the dose is to decrease the tube current; however, image noise at lower tube currents is greater than that at a higher tube current [8]. Because a normal myocardium is also contrast-enhanced, LIE-CT images reportedly show lower contrast than LGE-MRI [9]. The higher noise and lower contrast are the reasons for the lower CNR in LIE-CT in comparison with LGE-MRI. The sensitivities in the LIE-CT images were lower than those in the LGE-MR images [10]. This lower CNR is one reason for the lower sensitivity in LIE-CT.

To improve the CNR, a high contrast between the normal and the infarcted areas is important. An additional contrast medium injection with a slow injection rate improved image quality and showed good agreement with LGE-MRI findings in a porcine model [8]. The use of a bolus injection and an additional injection with a slow injection rate has also been reported in humans and has been useful in predicting LV functional recovery and wall thickness [11]. Therefore, we used an additional contrast medium injection with a slow injection rate in order to improve contrast. The CT value of the infarcted myocardium is reported to be the highest 5 min after bolus injection [8, 16]. In addition, a study using bolus and a slow injection protocol found that the contrast between LIE and the left ventricular cavity was significant at 3 and 5 min

after injection but not significant at 10 and 15 min after injection [8]. Therefore, the LIE-CT scan was performed 5 min after bolus injection in our study.

Acquiring an image at a low kVp value is also useful for improving contrast. Several studies of patients with chronic myocardial infarction reported that a low-kVp image had a higher accuracy than a mixed image or a high-kVp image [12, 13]. Our results are consistent with these studies. However, a low-kVp image also shows more noise than a high-kVp image [8]. Noise-reduction processing is useful to decrease the noise in low-kVp images. Our results showed that the CNR of the denoised low-kVp image was higher than that of the low-kVp image. Thus, the filter preserved the contrast between the normal and infarcted areas and effectively decreased the noise, producing improved CNR in the denoised low-kVp image.

The higher contrast obtained with a low kVp value and the noise reduction achieved by a denoise filter are the reasons for the high CNR in the denoised low-kVp image. The improved CNR enhances the diagnostic accuracy of these images. The denoised low-kVp image showed a good CNR (as an objective assessment) and favorable diagnostic accuracy (as a subjective assessment). The radiation dose of the denoised low-kVp image was lower than that of the mixed image. Therefore, this method enhanced diagnostic ability while maintaining a lower radiation dose.

Beam-hardening artifacts and streak artifacts are other factors that degrade diagnostic accuracy. These artifacts cannot be erased with a denoise filter. A recent study reports

that targeted spatial frequency filtration with image averaging is useful for decreasing streak artifacts [17]. An iodine map obtained from DECT is expected to have high accuracy in this regard. A study in a porcine model of chronic myocardial infarction reported that the diagnostic accuracy of the iodine map of LIE-CT (compared with the histopathological infarction) was greater than that of the 100-kVp images [10]. However, studies in human patients with chronic myocardial infarction have reported that the sensitivity and positive predictive value were lower for the iodine map of LIE-CT than for the 100-kVp images [12, 13]. In one of these same studies, the iodine map overestimated the volume of late enhancement compared to LGE-MRI [13].

There are some advantages to LIE-CT compared to LGE-MRI. First, CT can be performed in patients for whom MRI is contraindicated (e.g., those with metal implants, pacemakers, and claustrophobia). For patients with pacemakers or those with heart failure, LIE-CT is a useful method. Second, LIE-CT can obtain a whole heart image that can be reconstructed in any axis view. The number of LGE-MR images varies depending on mechanical performance and study time; the image may not include the whole heart. Third, CCTA is performed under this protocol and enables comprehensive assessment of coronary territories, coronary stenosis, and largeness of LIE. Fourth, the study time of CT is much shorter than that of MRI. Fifth, LGE-MRI requires skill for imaging (e.g., setting the inversion time). However, it is relatively easy to perform LIE-CT. Sixth, cardiac CT is more popular and is able to be performed in more hospitals compared to cardiac MRI. Thus, if LIE-CT is developed further, it will be useful for a larger pool of patients compared to its present use.

However, there are also some disadvantages of LIE-CT. First, LIE-CT emits a radiation dose. The radiation dose can be decreased by using a low kVp value and denoising processing (e.g., a filter or iterative reconstruction) with preserved diagnostic accuracy. Prospective ECG gating is also useful for decreasing the radiation dose. Second, LIE-CT requires additional contrast medium to preserve contrast. However, CCTA and LIE-CT enable the comprehensive assessment of coronary territories, coronary stenosis, and largeness of LIE. Third, LIE-CT images have a relatively low CNR, though this can be improved if the system is operated with a low kVp value and denoising processing.

These issues suggest that LIE-CT cannot completely replace LGE-MRI; however, it may be an alternative or an accessory technique. If LIE-CT can be carried out in the hospitals equipped to perform cardiac CT, patients who show LIE can be referred to hospitals that can perform cardiac MRI in order to undergo detailed examinations. Further studies are required to improve the CNR and sensitivity of this technique. Further studies on cardiac myopathies are also needed.

## Limitations

There are several limitations in this study. First, the number of patients was relatively small. Second, myocardial infarction was not assessed with histopathological findings. Third, because patients with AMI were recruited, a dynamic change in the days between LIE-CT and LGE-MRI cannot be ruled out.

## Conclusion

In conclusion, the use of a denoise filter with a low-kVp image improved the CNR of LIE-CT. Late iodine enhancement CT may be an alternative or an accessory technique for detecting late myocardial enhancement.

## Compliance with Ethical Standards

**Conflict of interest** Takuya Matsuda declares that he has no conflict of interest. Teruhito Kido declares that he has no conflict of interest. Toshihide Itoh is an employee of Siemens Japan. Hideyuki Saeki declares that he has no conflict of interest. Susumu Shigemi declares that he has no conflict of interest. Kouki Watanabe declares that he has no conflict of interest. Tomoyuki Kido declares that he has no conflict of interest. Shoji Aono declares that he has no conflict of interest. Masaya Yamamoto declares that he has no conflict of interest. Takeshi Matsuda declares that he has no conflict of interest. Teruhito Mochizuki declares that he has no conflict of interest.

**Ethical approval** All procedures performed in studies involving human participants were in accordance with the ethical standards of the institutional research committee and with the 1964 Helsinki declaration and its later amendments or comparable ethical standards.

**Informed consent** Informed consent was obtained from all individual participants included in the study.

## References

- Kim RJ, Fieno DS, Parrish TB, Harris K, Chen EL, Simonetti O, Bundy J, Finn JP, Klocke FJ, Judd RM (1999) Relationship of MRI delayed contrast enhancement to irreversible injury, infarct age, and contractile function. *Circulation* 100(19):1992–2002
- Kim RJ, Wu E, Rafael A, Chen EL, Parker MA, Simonetti O, Klocke FJ, Bonow RO, Judd RM (2000) The use of contrast-enhanced magnetic resonance imaging to identify reversible myocardial dysfunction. *N Engl J Med* 343(20):1445–1453
- Beek AM, Kuhl HP, Bondarenko O, Twisk JW, Hofman MB, van Dockum WG, Visser CA, van Rossum AC (2003) Delayed contrast-enhanced magnetic resonance imaging for the prediction of regional functional improvement after acute myocardial infarction. *J Am Coll Cardiol* 42(5):895–901
- Lee VS, Resnick D, Tiu SS, Sanger JJ, Nazzaro CA, Israel GM, Simonetti OP (2004) MR imaging evaluation of myocardial viability in the setting of equivocal SPECT results with (99 m)Tc sestamibi. *Radiology* 230(1):191–197
- Wagner A, Mahrholdt H, Holly TA, Elliott MD, Regenfus M, Parker M, Klocke FJ, Bonow RO, Kim RJ, Judd RM (2003) Contrast-enhanced MRI and routine single photon emission



- computed tomography (SPECT) perfusion imaging for detection of subendocardial myocardial infarcts: an imaging study. *Lancet* 361(9355):374–379
6. Raff GL, Gallagher MJ, O'Neill WW, Goldstein JA (2005) Diagnostic accuracy of noninvasive coronary angiography using 64-slice spiral computed tomography. *J Am Coll Cardiol* 46(3):552–557
  7. Miller JM, Rochitte CE, Dewey M, Arbab-Zadeh A, Niinuma H, Gottlieb I, Paul N, Clouse ME, Shapiro EP, Hoe J, Lardo AC, Bush DE, de Roos A, Cox C, Brinker J, Lima JA (2008) Diagnostic performance of coronary angiography by 64-row CT. *N Engl J Med* 359(22):2324–2336
  8. Brodoefel H, Klumpp B, Reimann A, Ohmer M, Fenchel M, Schroeder S, Miller S, Claussen C, Kopp AF, Scheule AM (2007) Late myocardial enhancement assessed by 64-MSCT in reperfused porcine myocardial infarction: diagnostic accuracy of low-dose CT protocols in comparison with magnetic resonance imaging. *Eur Radiol* 17(2):475–483
  9. Nieman K, Shapiro MD, Ferencik M, Nomura CH, Abbara S, Hoffmann U, Gold HK, Jang IK, Brady TJ, Cury RC (2008) Reperfused myocardial infarction: contrast-enhanced 64-Section CT in comparison to MR imaging. *Radiology* 247(1):49–56
  10. Deseive S, Bauer RW, Lehmann R, Kettner M, Kaiser C, Korkusuz H, Tandl C, Theisen A, Schachinger V, Schoepf UJ, Vogl TJ, Kerl JM (2011) Dual-energy computed tomography for the detection of late enhancement in reperfused chronic infarction: a comparison to magnetic resonance imaging and histopathology in a porcine model. *Invest Radiol* 46(7):450–456
  11. Koyama Y, Matsuoka H, Mochizuki T, Higashino H, Kawakami H, Nakata S, Aono J, Ito T, Naka M, Ohashi Y, Higaki J (2005) Assessment of reperfused acute myocardial infarction with two-phase contrast-enhanced helical CT: prediction of left ventricular function and wall thickness. *Radiology* 235(3):804–811
  12. Srichai MB, Chandarana H, Donnino R, Lim II, Leidecker C, Babb J, Jacobs JE (2013) Diagnostic accuracy of cardiac computed tomography angiography for myocardial infarction. *World J Radiol* 5(8):295–303
  13. Wichmann JL, Bauer RW, Doss M, Stock W, Lehnert T, Bodelle B, Frellesen C, Vogl TJ, Kerl JM (2013) Diagnostic accuracy of late iodine-enhancement dual-energy computed tomography for the detection of chronic myocardial infarction compared with late gadolinium-enhancement 3-T magnetic resonance imaging. *Invest Radiol* 48(12):851–856
  14. Black MJ, Sapiro G, Marimont DH, Heeger D (1998) Robust anisotropic diffusion. *IEEE Trans Image Process* 7(3):421–432
  15. Cerqueira MD, Weissman NJ, Dilsizian V, Jacobs AK, Kaul S, Laskey WK, Pennell DJ, Rumberger JA, Ryan T, Verani MS (2002) Standardized myocardial segmentation and nomenclature for tomographic imaging of the heart. A statement for healthcare professionals from the Cardiac Imaging Committee of the Council on Clinical Cardiology of the American Heart Association. *Circulation* 105(4):539–542
  16. Lardo AC, Cordeiro MA, Silva C, Amado LC, George RT, Saliaris AP, Schuleri KH, Fernandes VR, Zviman M, Nazarian S, Halperin HR, Wu KC, Hare JM, Lima JA (2006) Contrast-enhanced multidetector computed tomography viability imaging after myocardial infarction: characterization of myocyte death, microvascular obstruction, and chronic scar. *Circulation* 113(3):394–404
  17. Kurobe Y, Kitagawa K, Ito T, Kurita Y, Shiraishi Y, Nakamori S, Nakajima H, Nagata M, Ishida M, Dohi K, Ito M, Sakuma H (2014) Myocardial delayed enhancement with dual-source CT: advantages of targeted spatial frequency filtration and image averaging over half-scan reconstruction. *J Cardiovasc Comput Tomogr* 8(4):289–298